Available online at www.sciencedirect.com
ScienceDirect
Journal of Power Sources 171 (2007) 517–523
JOURNAL OF POWER SOURCES
www.elsevier.com/locate/jpowsour

Short communication

The use of the heteropoly acids, $H_5PMo_{10}V_2O_{40}$, $H_7[P_2W_{17}O_{61}(Fe^{III}\cdot OH_2)]$ or $H_{12}[(P_2W_{15}O_{56})_2Fe_4{}^{III}(H_2O)_2]$, in the anode catalyst layer of a proton exchange membrane fuel cell

Mei-Chen Kuo [a], Bradford R. Limoges [a], Ronald J. Stanis [a,b], John A. Turner [b], Andrew M. Herring [a,*]

[a] *Department of Chemical Engineering, Colorado School of Mines, Golden, CO 80401, United States*
[b] *Hydrogen and Electricity Systems and Infrastructure Group, National Renewable Energy Laboratory, Golden, CO 80401, United States*

Received 20 April 2007; received in revised form 12 June 2007; accepted 12 June 2007
Available online 23 June 2007

Abstract

The use of heteropoly acids (HPAs) in PEM fuel cell anode catalyst layers was studied. To compare the doped electrodes with a control electrode in a meaningful way membrane electrode assemblies (MEAs) were prepared with two 1/2 anodes, one the undoped control and one the test electrode. This ensured that both the control and test electrode were subject to the same thermal and electrochemical history. After curve fitting the data using a least squares method the error was found to be 1% in E_0, 25% in the Tafel slope and 15% in the area specific resistance. The electrodes used were commercial electrodes of the Los Alamos type (ELATs). Doping a fuel cell anode with $H_5PMo_{10}V_2O_{40}$ resulted in a fourfold increase in the area specific resistance of the MEA, but the performance was not equivalent to that of an anode incorporating Nafion®. Doping $H_5PMo_{10}V_2O_{40}$ in Nafion® painted ELATs resulted in negligible improvements in the performance compared to ELATs incorporating only Nafion®. Much more impressive was the improvement in maximum power from doping the Nafion® painted ELAT with $H_7[P_2W_{17}O_{61}(Fe^{III}\cdot OH_2)]$ or $H_{12}[(P_2W_{15}O_{56})_2Fe_4{}^{III}(H_2O)_2]$. Eighty-five percent improvements in maximum power and 100% improvements in area specific resistance were observed from this HPA doped ELAT.

Keywords: PEM fuel cell; Gas diffusion electrode; Heteropoly acid; Interfacial resistance; Anode

1. Introduction

The proton exchange membrane (PEM) fuel cell holds much promise as an efficient and versatile energy conversion device. However, in order for the PEM fuel cell to achieve widespread usage a number of key technical hurdles need to be overcome. These include the discovery of an efficient $4e^-$ oxygen reduction reaction (ORR) electrocatalyst, an anode catalyst that is at least as efficient as Pt for the hydrogen oxidation reaction (HOR) and is not easily poisoned by small molecules such as carbon monoxide, and a fuel cell membrane that can be operated at elevated temperatures without the need for external humidification for adequate proton conduction. For any or all of these approaches to succeed the catalyst/ionomer/electron conducting three-phase boundary must be engineered for maximum performance. The optimal design of the catalyst layer in the electrode is, therefore crucial, to the performance of the fuel cell.

In a conventional PEM fuel cell the perflourosulfonic acid (PFSA) PEM is attached to a platinum catalyzed anode on the hydrogen (fuel) side of the cell and a platinum catalyzed cathode on the oxygen (air) side of the cell. The platinum is supported on an electrically conductive high surface area carbon which is coated with the ionomer to fabricate a three-phase boundary, between proton conductor (ionomer), electron conductor and reactant gases. The standard ionomer in use in PEM fuel cells is a PFSA polymer such as Nafion® [1]. While much is known about the effect of PFSA ionomer loading and equivalent weight on the electrode performance in terms of ionic conductivity and porosity [2–4], very little is known about the use of other proton conducting materials in the PEM fuel cell catalyst

* Corresponding author. Tel.: +1 303 384 2082; fax: +1 303 273 3730.
E-mail address: aherring@mines.edu (A.M. Herring).

0378-7753/$ – see front matter © 2007 Elsevier B.V. All rights reserved.
doi:10.1016/j.jpowsour.2007.06.063

layer [5]. In fact most catalyst layers with new membranes contain Nafion® as the sole ionomer, although a patent proposing inorganic proton conducting materials has been granted [6]. The use of zirconium hydrogen phosphate in fuel cell electrodes has been shown to be beneficial to high temperature operation [7]. Such studies are important because they shed light on transport phenomena in the catalyst layer and point to new materials for enhanced performance. It will also be necessary to develop new ionomers for the catalyst layers in PEM fuel cells to utilize many of the promising novel proton conducting polymers [8] and composite materials [9] currently being developed. A thorough understanding of transport in the catalyst layer and proton transport from the catalyst layer to the PEM is essential to avoid large interfacial resistances in the fuel cell.

The heteropoly acids (HPAs) represent a class of inorganic proton conductors that also have interesting redox properties. The HPA and the zirconyly phosphates have been proposed as the proton conductor in PEM fuel cell catalyst layers [6,7]. Some HPAs have proton conductivities as high as $0.2\,S\,cm^{-1}$ representing some of the highest known proton conductivities measured in the solid state [10,11]. When reduced, the HPAs also become capable of electron conduction giving rise to a mixed electronic/protonic conductor. Such a material could dramatically improve electronic and protonic conduction in the fuel cell anode. We have been studying a number of different HPA in the solid state and their impact on the performance of the fuel cell membrane electrode assembly (MEA) in the absence of platinum [12,13]. In this paper we now report on the use of HPAs in the anode layer of the PEM fuel cell MEA as a mixed protonic/electronic conducting additive in the PFSA platinum containing catalyst layer.

For this study we focused on a series of iron substituted HPA based on the Wells–Dawson structure [14]. The iron substituted HPA are interesting catalysts [15,16] and electro-catalysts [17,18]. Our original thought was that they would enhance the hydrogen oxidation reaction (HOR), but as the HOR on Pt is extremely rapid [19] it is much more likely that the observed effects are on proton and electron transport away from the catalyst and into the ionomer and current collector of the electrode layer. The Wells–Dawson HPA $[(X^{n+})_2M_{18}O_{62}]^{2n-16}$, where X^{n+} represents a central atom such as, P^{5+}, As^{5+}, or S^{6+}; surrounded by a cage of M addenda atoms, such as W^{6+} or Mo^{6+}, arranged in MO_6 octahedral units. The structure, of the α isomer, possesses two identical "half units" with the central atom surrounded by nine octahedral units XM_9O_{31} linked through oxygen atoms [20]. Non-saturated compounds such as, $XW_{11}O_{39}{}^{n-12}$ and $X_2W_{17}O_{61}{}^{2n-}$, called "lacunary" species are synthesized through the degradation of the Wells–Dawson anions in controlled basic media [20]. Iron may be substituted in the monolacunary HPA to yield $[P_2W_{17}O_{61}(Fe^{III}{\cdot}OH_2)]^{7-}$ but when substitution in the tri-lacunary HPA, the Wells–Dawson sandwich compound $[(P_2W_{15}O_{56})_2Fe_4{}^{III}(H_2O)_2]^{12-}$ is obtained, Fig. 1. Both of these HPA were isolated as the sodium salt and converted to the free acid by extraction from acid solution as the ether adduct. As the ether was not cooled the Wells–Dawson sandwich molecule had only two iron atoms [12]. We also report some preliminary data for Keggin HPA $H_5PMo_{10}V_2O_{40}$, not shown.

Small amounts of HPA are strongly adsorbed on to carbons. Such adsorbed HPA survive washing with water, necessary for removal of loosely bound HPA, and are robust enough that an MEA containing them can be brought to steady state and thoroughly studied for several days. In order to compare the HPA doped anode to the undoped anode control we prepared MEAs with both electrodes on the anode side. This ensured that each electrode was subjected to the same fabrication history and was conditioned to steady state under the same conditions. By use of a masked gasket we were able to independently measure each electrode to achieve a qualitative comparison.

2. Experimental

2.1. Materials

The HPAs, K_7 or $H_7[(P_2W_{17}O_{61})Fe^{III}(H_2O)]$ (KFe1, HFe1) and Na_{12} or $[(P_2W_{15}O_{56})_2Fe_4{}^{III}(H_2O)_2]$ and its disubstituted free acid analogue (NaFe4 and HFe2) were prepared and characterized as described previously [12,16]. α-$H_3P_2W_{18}O_{62}$ (Wells–Dawson) and $H_5PMo_{10}V_2O_{40}$ (HV2) was prepared by literature methods [21,22]. The number of waters associated with each HPA was determined by thermogravimetric analysis using a TGA/DTA 220 analyzer (Seiko Instruments Inc.) under He at 10 psi a from 25 to 300 °C at a rate of $5\,°C\,min^{-1}$.

The gas diffusion electrode (GDE) used was a single sided electrode Los Alamos type (ELAT) (E-Tek, De Nora, NA) loaded at $0.5\,mg\,cm^{-2}$ Pt (20% Pt on Vulcan XC-72 carbon). GDEs were cleaned with boiling DI water and 3% H_2O_2 solution before use. The HPA doped GDEs were prepared as described previously for a doped GDL giving a typical loading of typically $0.04\,mg\,cm^{-2}$ [12]. Nafion® 117 (Ion Power) was washed in successive boiling solutions of 3% H_2O_2, DI water, 0.5 M H_2SO_4, and DI water each for 1 h.

2.2. Preparation of split anode MEA

MEAs were prepared in the configuration shown in Fig. 2. The MEA was fabricated with a HPA doped Pt GDE (about $2.2\,cm^2$), and a Pt control GDE (about $2.2\,cm^2$), separated by a small gap on the anode and a larger Pt GDE ($5\,cm^2$) on the cathode. The electrodes were hand painted with Nafion® solution (approx. loading: $1.8\,mg\,cm^{-2}$) and allowed to dry in the air. The electrodes were then pressed on to a Nafion® 117 membrane with a digital combo multi-purpose press (GEO Knight & Co. Inc.) at 115 °C and 80 psi for 90 s.

2.3. Measurements

Fuel cell measurements were made in $5\,cm^2$ active area hardware (fuel cell technologies) at 80 °C using saturated H_2 and O_2 (99.999%, general air) at 100% RH, humidifier (Lyntech Industries, Inc., FCTS BH) 90 °C dew-point. The gasses were metered at a flow rate $0.1\,l\,min^{-1}$ of H_2 and O_2 with 30 psi backpressure (Lynntech Industry, Inc., FCTS GMET/H). The fuel cells were either tested against an electronic load (Lynntech Industries, Inc.,

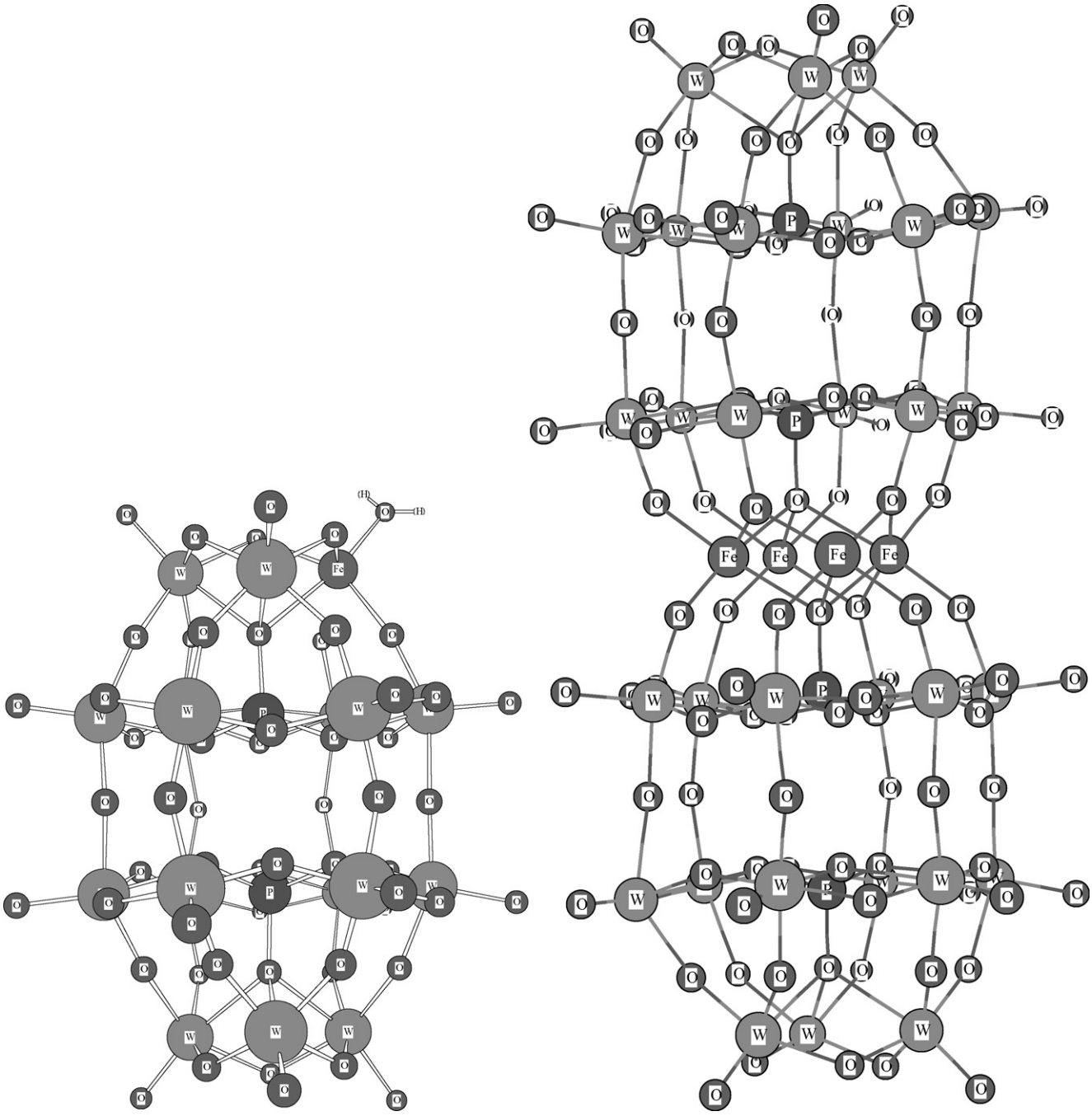

Fig. 1. Stylized representation of left, $[(P_2W_{17}O_{61})Fe^{III}(H_2O)]^{7-}$ (KFe1 or HFe1) in which one W–O octahedron from the crystal structure of the $[P_2W_{18}O_{62}]^{6-}$ [14] has been replaced by an $Fe^{III}(OH_2)$ moiety and crystal structure of $[(P_2W_{15}O_{56})_2Fe_4{}^{III}(H_2O)_2]^{12-}$ (NaFe4 or with 2Fe removed HFe2) [16].

FCTS EL,) using FC Power^{TM} or a potentiostat (Arbin Instruments, Austin, TX, BT 4+) using MITS PRO^{TM} software. All MEAs were conditioned in the following manner: the potential was held at 0.6 V for 1 h, followed by cycling between 0.7 and 0.5 V for 1/2 h at each potential until the average current reached steady state, normally 12 h. The MEA was removed from the cell and the anode gasket was replaced with a 2.2 cm^2 sized gaskets that covered one of the two half-anode GDEs. The gasket provides two purposes: one is to seal the cell allowing back pressure of gasses, and the second is to provide electrical insulation between one of the GDEs and the anode graphite plate. When the appropriate half-anode GDE has been tested, the MEA was removed and the half-anode gasket was rotated 180° to allow access to the other half-anode GDE. Polarization curves were fitted using Igor Pro.

3. Results and discussion

3.1. Error analysis

The primary drawback in the study of experimental MEAs in fuel cells is that the reproducibility of the MEA fabrication

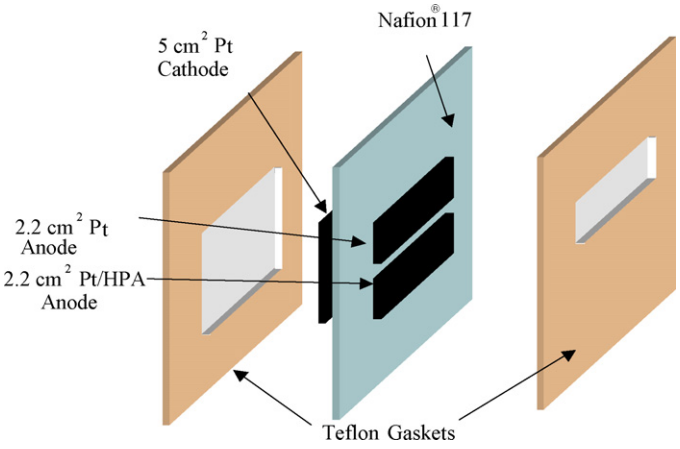

Fig. 2. Schematic diagram of split anode MEA configuration and gasket design.

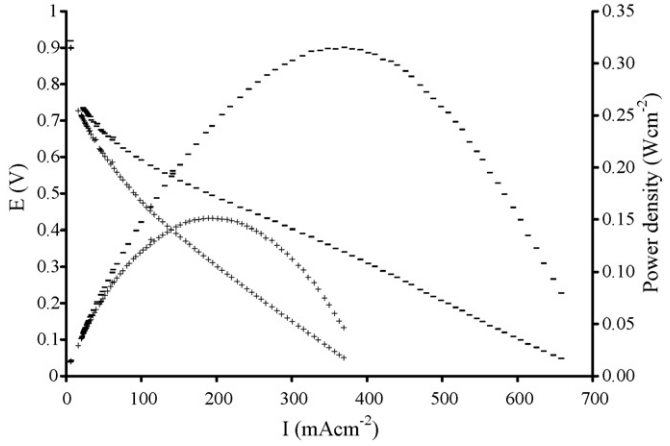

Fig. 3. Polarization and power curves for + (lower) Pt control anode and – $H_5PMo_{10}V_2O_{40}$ doped Pt anode with no added Nafion® in anode electrode layers.

can vary considerably between MEAs. Because the history of a MEA from fabrication to steady state operation may vary, the error may be unacceptable. Using fairly sophisticated MEA fabrication techniques we have eliminated many of these errors [23]. This paper, however, is concerned with a method to rapidly screen catalyst layer additives on prefabricated ELAT electrodes. Our solution to the reproducibility issue was to fabricate an MEA where the control electrodes and the test electrode were on the same MEA, Fig. 2. This approach ensured that both electrodes were subject to the same fabrication and conditioning conditions. A direct comparison of the control and test electrodes is then possible. For each additive tested, enough MEAs were fabricated so that least two MEAs with acceptable performance could be used for the purposes of data reporting. The errors reported for V_{oc}, I at 0.2 V and ΔP are from these duplicate measurements.

It would be expected that the polarization curves for all the controls should be identical. In fact they are not and this reflects the variability in MEA fabrication and conditioning. To further analyze the variability of these MEAS we fit the polarization curves by a nonlinear least square fitting procedure [2] using Eq. (1) of the form:

$$E = E_0 - b \log i - R_i i \quad (1)$$

where

$$E_0 = E_{V_{oc}} + b \log i_0 \quad (2)$$

which is effectively the cell potential at 1 mA and is a quantitative measure of the cathode electrode kinetics, b is the Tafel slope, and R_i is the differential resistance of the cell. From this analysis we get the following values for the control data; $E_0 = 0.95 \pm 0.01$ V, $b = 80 \pm 10$ mV decade^{-1}, and $R_i = 0.35 \pm 0.05$ mΩ cm^{-2}. Even though the error in E_0 was only 1% all the test MEAs were within this error and so E_0 was not affected. For the Tafel slope, the error was 25%, but, with only two exceptions was an improvement greater than this observed. A 15% error was observed in R_i. Table 1 lists the values of R_i for all of the experimental MEAs as improvements greater than 15% in R_i were observed for almost all of the HPA anode doped MEA.

3.2. MEAs without added Nafion® ionomer

Initial investigations focused on replacing the Nafion® ionomer with the small amounts of HPA that can be strongly adsorbed on the ELAT. As expected the performance of the Pt control with no ionomer in the anode catalyst layer, Fig. 3, is rather poor. At 0.2 V the current density is only 350 mA cm^{-2} and the maximum power obtained is 0.14 W cm^{-2}. We can compare this to a typical MEA with Nafion® painted on to both catalyst layers, Fig. 8. For this MEA, at 0.2 V the current density is 1.1 A cm^{-2} and the maximum power obtained is 0.35 W cm^{-2}.

Table 1
Data for the Pt control and HPA doped Pt test half MEAs

Compound	V_{oc} (mV)	I at 0.2 V (mA cm^{-2})	P (W cm^{-2})	ΔP (%)	Area resistance (Ω cm^{-2})	ΔArea resistance (%)	Dominant effect
Wells–Dawson	944 ± 15	1460 ± 2%	0.45	16 ± 3	0.32	−17	Anode
Pt	926 ± 17	1320 ± 3%	0.387		0.27		
KFeP2W	943 ± 19	1520 ± 1%	0.42	57 ± 6	0.31	14	Anode/transport
Pt	959 ± 25	951 ± 5%	0.267		0.36		
HFeP2W	961 ± 14	1510 ± 2%	0.536	65 ± 1	0.25	50	IR
Pt	925 ± 11	1100 ± 1%	0.324		0.38		
NaFe4P4W	969 ± 21	1580 ± 4%	0.505	46 ± 3	0.28	47	IR/transport
Pt	938 ± 19	1050 ± 3%	0.346		0.41		
HFe2P4W	958 ± 16	1980 ± 3%	0.679	85 ± 2	0.17	100	IR
Pt	923 ± 18	1130 ± 1%	0.367		0.25		

Some of this performance can be recovered by the use of an HPA adsorbed on to the carbon of the ELAT. The data for the 1/2 anode doped with the divandium substituted HPA HV2 on the same MEA is also shown in Fig. 3. For this HV2 doped MEA at 0.2 V the current density is 500 mA cm^{-2} and the maximum power obtained is 0.31 W cm^{-2}, close to that of the half anode with added Nafion®. Curve fitting of the polarization curves revealed no difference in E_0 and the Tafel slope within the experimental error. A factor of 4.3 improvement was observed in R_i from 0.9 mΩ cm^{-2} in the undoped Pt control ELAT to 0.22 ± 0.03 mΩ cm^{-2} in the HV2 doped Pt ELAT. This is a somewhat remarkable result considering that the typical loading of HPA that we obtain on an ELAT is ca. 0.04 mg cm^{-2} which represents a molar loading of ca. 1 μmol cm^{-2} [12,13]. We postulate that proton transport in this system is through the liquid water on the surface of the carbon as the anode gases are saturated with water vapor. The HPA obviously lowers the activation barrier for proton transport which is manifested in a dramatically improved area specific resistance of the cell. The HPA on the anode is almost certainly in a reduced form and so an additional effect on electronic transport is also possible. Additionally, as there is no added Nafion® in this electrode it is possible that gas transport is also facilitated. No attempt was made to separate these effects, but all are probably in play. Even though impressive improvements in the interfacial resistance of the fuel cell can be achieved solely with HPAs, the performance does not match that of the Nafion® coated electrode. We therefore decided to see if we could improve an electrode with added Nafion®.

3.3. Enhancements to MEAs with added Nafion® ionomer

The improvements seen in the performance of an MEA using Nafion® doped electrodes with HV2 were not statistically greater than the controls. This was not true for some Fe substituted HPAs. The polarization and power curves for a control Pt anode and a HFe2 doped Pt anode with Nafion® are shown in Fig. 8.

The performance of the control MEA with Nafion® added to both electrodes is quite impressive, with 1.13 A cm^{-2} at 0.2 V and a maximum power of 0.367 W cm^{-2}, Table 1. This is comparable to reported values for MEAs using Nafion® 117 as the membrane [24]. However the MEAs and fuel cells in this study were not fully optimized [25,26], but importantly were measured under the same conditions to ensure that the results were reproducible. The intent was that MEA optimization would occur with candidate materials identified by the study at a later time. What is interesting is the dramatic improvement in the performance of the MEA when the anode is doped with the Wells–Dawson sandwich HPA HFe2. For this HPA doped MEA the current improves to 1.98 A cm^{-2} at 0.2 V and the maximum power observed is 0.679 W cm^{-2}, Table 1. This represents an improvement in power of 85%. When the polarization curves are fit by the method described above, we see that we have obtained a 100% decrease in the area specific resistance of the MEA by the addition of ca. 1 μMol cm^{-2} HFe2 HPA.

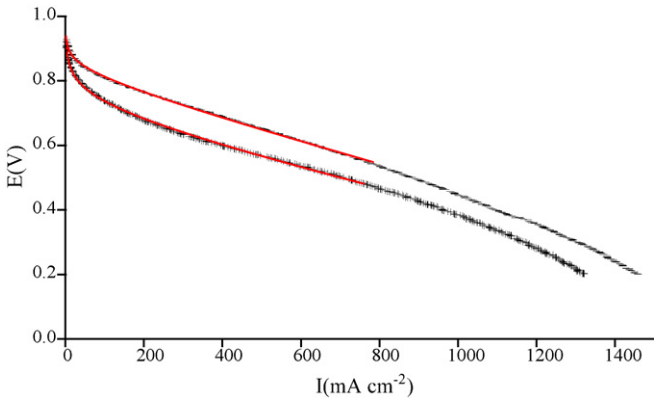

Fig. 4. Polarization curves and curve fit lines for + (lower) Pt control anode and − Wells–Dawson doped Pt anode with added Nafion® in anode electrode layers.

In order to determine how these relative small amounts of HPA were improving the performance of the fuel cell anode layer we doped a number of MEA anodes with a series of related HPAs, Table 1. The Wells–Dawson and iron substituted HPA studied here were all shown to be poor catalysts for the HOR [12]. Therefore, any enhancement to the performance of the Pt catalyzed fuel cell anode will be because the HPA are facilitating the transport of reactants or products. The control Pt and Wells–Dawson doped anode data and curve fits are shown in Fig. 4. Doping of the fuel cell anode with the parent Wells–Dawson HPA showed ca. 15% improvement in power. The fitted curve showed a decrease in area specific resistance. This decrease in area specific resistance is approximately the same as the error in the measurement and so we conclude that there was no change due to this HPA. However, inspection of Fig. 4 shows that the Wells–Dawson HPA doped anode MEA has a higher current density. The fitted Tafel slope did improve to 51 mV $decade^{-1}$. While the polarization curve is dominated by the cathode polarization, the anode polarization is still a contributing factor and so the Wells–Dawson HPA clearly is improving the effective catalytic rate of the anode hydrogen oxidation reaction, and this does manifests itself in an improvement in maximum power of the MEA.

Doping the anode with the mono-iron salt KFeP2W, Fig. 5. Produced a significant improvement in the power of the MEA by

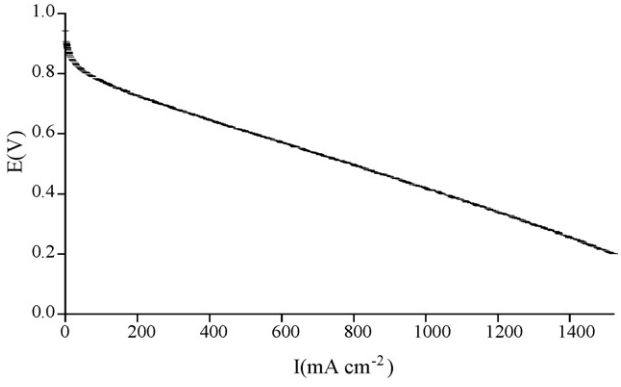

Fig. 5. Polarization curve for − KFeP2W doped Pt anode with added Nafion® in anode electrode layers.

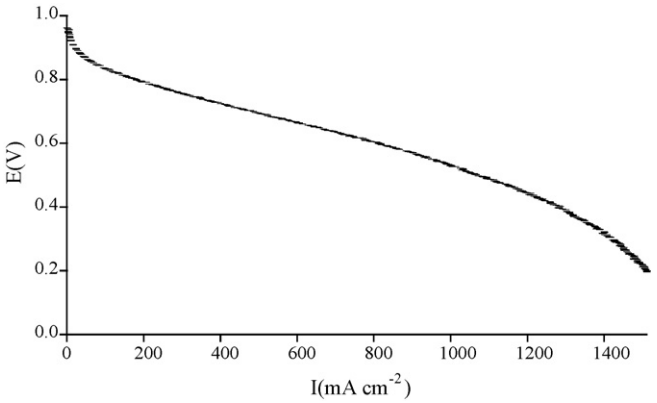

Fig. 6. Polarization curve for − HFeP2W doped Pt anode with added Nafion® in anode electrode layers.

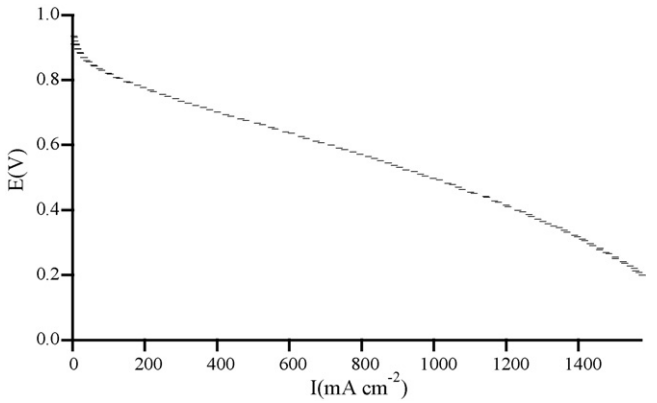

Fig. 7. Polarization curve for − NaFe4P4W doped Pt anode with added Nafion® in anode electrode layers.

57%, Table 1. An improvement was again seen in the fitted Tafel slope, 60 mV decade^{-1}, due to an improvement in the overall anode catalysis, but, again no significant improvement in the area specific resistance. Examination of the polarization curve shows no deviation due to concentration limitations, which is seen for all the free acid HPAs and control Pt MEAs at <0.4 V. The improvement in power observed here is, therefore, due to an improvement in ion transport enhanced by the HPA.

We next doped the Nafion® painted ELAT with the free acid of the mono-iron HPA, HFeP2W, Fig. 6, Table 1. This doped MEA had an even larger increase in maximum power, 65%, but as with the other free acid HPAs there was an obvious transport loss at <0.4 V. We can see this when we compare the current density of the free acid at 0.2 V, 1.51 A cm^{-2}, with that of the lower power potassium salt discussed above 1.52 A cm^{-2}, which is the same value within experimental error. The higher performing free acid does suffer a loss of transport polarization due to inadequate gaseous transport in the catalyst layer. However, when we examine the parameters from the curve fit we see that there is no change in Tafel slope, but, there is a significant improvement in the area specific resistance of 50%.

There appeared to be an effect on performance that correlated with the number of iron atoms in the HPA, so a Nafion® painted ELAT doped with the sodium salt of the tetra-iron Wells–Dawson sandwich HPA, NaFe4P4W (Fig. 7, Table 1). This HPA showed a more modest improvement in maximum power of 46%, but again as with the potassium salt of the mono-iron HPA, KFeP2W, there was a small evident loss in concentration polarization at <0.4 V, the current density at 0.2 V being an improved 1.58 A cm^{-2}. The fitted data showed no change in Tafel slope but a 47% improvement in area specific resistance.

We prepared the free acid of NaFe4P4W at room temperature, this meant that the free acid of the HPA that we obtained had lost 2 Fe atoms (the tetra substituted HPA is available by preparing the free acid under ice cold conditions). We decided to use HFe2P4W as it would presumably be more robust under fuel cell operating conditions. The doping of the Nafion® painted ELAT with this HPA produced the most impressive improvements, Table 1 and Fig. 8. The maximum power is improved by 85% and the current density at 0.2 V is an impressive 1.98 A cm^{-2}.

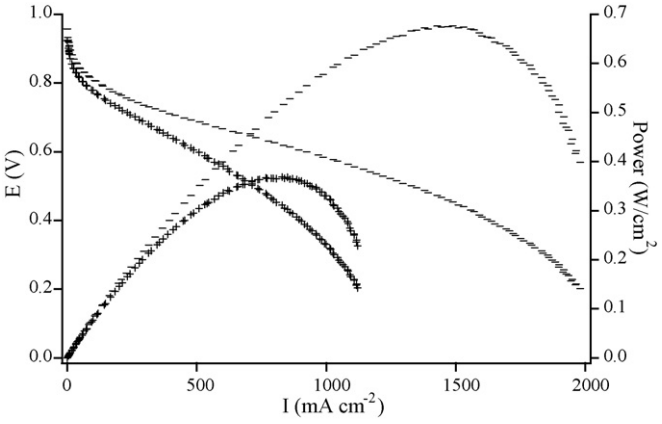

Fig. 8. Polarization and power curves for + (lower) Pt control anode and − HFe2 doped Pt anode with added Nafion® in anode electrode layers.

All of this improvement is due to a 100% increase in the area specific resistance of the MEA, there being no improvement to the Tafel slope from the curve fitted data.

More detailed studies will be required to fully rationalize the trends in this data, however we may draw some conclusions based on structural arguments. None of the HPA are present in large enough amounts to come even close to forming a monolayer or to be regarded as having connectivity throughout the catalyst layer. These HPA are present in catalytic amounts, i.e. they are lowering the activation barrier for electrode processes through their interaction with the ionomer and carbon. Statistically very small amounts of the HPA might be in electrochemical contact with the Pt catalyst.

TGA analysis of the materials, Table 2, shows that all have strongly bound water associated with them. The Wells–Dawson

Table 2
TGA data in equivalents of water lost with temperature for the HPA studied

Compound	≤100 °C	100–200 °C	≥200 °C
$K_7FeP_2W_{17}O_{61}$	8	6	1
$H_7FeP_2W_{17}O_{61}$	7	7	2
$Na_{12}Fe_4P_4W_{30}O_{112}$	26	8	4
HFe2P4W	23	10	6

sandwich HPA, HFe2P4W and NaFe4P4W have significantly more water associated with them than the monosubstituted HPA. Note that the water molecules observed to leave the structures above 200 °C are associated with loss of structural integrity of the HPA and not waters originally in the structure. The HPA are known to be super acids and the salts of HPA are usually not fully stoichiometric. That is to say the salts usually include some residual protons. The IR data of all the HPA and their salts studied, not shown, show δ(OH) 1630 and 1710 cm^{-1} associated with H_3O^+ and $H_5O_2^+$, respectively, to temperatures >200 °C. From this we conclude that there are residual protons even in the salts of the HPA. We expect the inclusion of Fe atoms in the HPA to increase its ease of being reduced and so the possibility of mixed electronic and protonic conductivity.

4. Conclusions

In Table 1 we summarize the dominant effect of each of the HPA dopants on the performance of the MEA. The first point to make is that none of the HPAs poison the anode catalyst, and in fact the Wells–Dawson parent and the mono-iron salt, KFeP2W, show a slight increase in improving the anode catalysis. The HOR is very fast [19] and it is unlikely that these HPA are actually increasing the rate of the HOR, rather the HPA are increasing the effective diffusion coefficient of species to the catalyst particle. Three of the HPA dramatically improve the area specific resistance of the MEA. HFeP2W, NaFe4P4W, and HFe2P2W appear to improve the protonic and by inference the electronic conduction in the catalyst layer. The improvements in maximum power scale in the order of increasing protons associated with the HPA, i.e. NaFe4P4W < HFeP2W < HFe2P2W. This is not surprising as HPA dopants are known to improve the proton conductivity of Nafion® [27–31]. This is clearly the dominant effect as the greatest improvement is seen with HFe2P2W which acts to increase interfacial protonic conduction. Finally the two HPA salts KFeP2W and NaFe4P4W also appear to improve transport in the MEA as little concentration polarization is observed in the polarization curves of these HPA at low V.

Acknowledgments

We would like to thank Excel Energy for a grant from the Renewable Development Fund.

References

[1] A.M. Herring, in: S. Lee (Ed.), Encyclopedia of Chemical Processing, vol. 2, Marcel Dekker, New York, 2006, p. 1085.
[2] E.A. Ticianelli, C.R. Derouin, A. Redondo, S. Srinivasan, J. Electrochem. Soc. 135 (1988) 2209.
[3] M. Uchida, Y. Aoyama, N. Eda, A. Ohta, J. Electrochem. Soc. 142 (1995) 4143.
[4] Z. Siroma, T. Sasakura, K. Yasuda, M. Azuma, Y. Miyazaki, J. Electroanal. Chem. 546 (2003) 73.
[5] E.B. Easton, T.D. Astill, S. Holdcroft, J. Electrochem. Soc. 152 (2005) A752.
[6] G. Alberti, M. Casciola, E. Ramunni, J. Rube, US patent 7,144,652, 2006.
[7] Z. Xie, T. Navessin, Z. Shi, R. Chow, S. Holdcroft, J. Electroanal. Chem. 596 (2006) 38.
[8] S.J. Hamrock, M.A. Yandrasits, Polym. Rev. 46 (2006) 219.
[9] A.M. Herring, Polym. Rev. 46 (2006) 245.
[10] K.D. Kreuer, M. Hampele, K. Dolde, A. Rabenau, Solid State Ionics 28–30 (1988) 589.
[11] A. Hardwick, P.G. Dickens, R.C.T. Slade, Solid State Ionics 13 (1984) 345.
[12] M.-C. Kuo, R.J. Stanis, J.R. Ferrell Iii, J.A. Turner, A.M. Herring, Electrochim. Acta 52 (2007) 2051.
[13] B.R. Limoges, R.J. Stanis, J.A. Turner, A.M. Herring, Electrochim. Acta 50 (2005) 1169.
[14] B. Dawson, Acta Cryst. 6 (1953) 113.
[15] X. Zhang, T.M. Anderson, Q. Chen, C.L. Hill, Inorg. Chem. 40 (2001) 418.
[16] X. Zhang, Q. Chen, D.C. Duncan, C.F. Campana, C.L. Hill, Inorg. Chem. 36 (1997) 4208.
[17] J.E. Toth, J.D. Melton, D. Cabelli, B.H.J. Bielski, F.C. Anson, Inorg. Chem. 29 (1990) 1952.
[18] J.E. Toth, F.C. Anson, J. Am. Chem. Soc. 111 (1989) 2444.
[19] S. Chen, A. Kucernak, J. Phys. Chem. B 108 (2004) 13984.
[20] L.E. Briand, G.T. Baronetti, H. Thomas, J. Appl. Catal. A: Gen. 256 (2003) 37.
[21] G.A. Tsigdinos, C.J. Hallada, Inorg. Chem. 7 (1968) 437.
[22] A.H. Cowley (Ed.), Inorganic Syntheses, vol. 31, Wiley, 1996.
[23] R.J. Stanis, M.C. Kuo, J.A. Turner, A.M. Herring, J. Electrochem. Soc., submitted for publication.
[24] S. Slade, S.A. Campbell, T.R. Ralph, F.C. Walsh, J. Electrochem. Soc. 149 (2002) A1556.
[25] W.-k. Lee, C.-H. Ho, J.W. Van Zee, M. Murthy, J. Power Sources 84 (1999) 45.
[26] J. Ge, A. Higier, H. Liu, J. Power Sources 159 (2006) 922.
[27] V. Ramani, H.R. Kunz, J.M. Fenton, J. Membr. Sci. 266 (2005) 110.
[28] V. Ramani, H.R. Kunz, J.M. Fenton, J. Power Sources 152 (2005) 182.
[29] V. Ramani, H.R. Kunz, J.M. Fenton, Electrochim. Acta 50 (2005) 1181.
[30] O. Savadogo, J. Power Sources 127 (2004) 135.
[31] S. Malhotra, R. Datta, J. Electrochem. Soc. 144 (1997) L23.